Singlet Oxygen-Induced Membrane Disruption and Serpin-Protease Balance in Vacuolar-Driven Cell Death[1][OPEN]

Eugene Koh, Raanan Carmieli, Avishai Mor, and Robert Fluhr*

Department of Plant and Environmental Sciences, Weizmann Institute, Rehovot, Israel (E.K., A.M., R.F.); and Department of Chemical Research Support, Weizmann Institute, Rehovot, Israel (R.C.)

ORCID ID: 0000-0003-1073-0050 (E.K.).

Singlet oxygen plays a role in cellular stress either by providing direct toxicity or through signaling to initiate death programs. It was therefore of interest to examine cell death, as occurs in Arabidopsis, due to differentially localized singlet oxygen photosensitizers. The photosensitizers rose bengal (RB) and acridine orange (AO) were localized to the plasmalemma and vacuole, respectively. Their photoactivation led to cell death as measured by ion leakage. Cell death could be inhibited by the singlet oxygen scavenger histidine in treatments with AO but not with RB. In the case of AO treatment, the vacuolar membrane was observed to disintegrate. Concomitantly, a complex was formed between a vacuolar cell-death protease, RESPONSIVE TO DESSICATION-21 and its cognate cytoplasmic protease inhibitor ATSERPIN1. In the case of RB treatment, the tonoplast remained intact and no complex was formed. Over-expression of AtSerpin1 repressed cell death, only under AO photodynamic treatment. Interestingly, acute water stress showed accumulation of singlet oxygen as determined by fluorescence of Singlet Oxygen Sensor Green, by electron paramagnetic resonance spectroscopy and the induction of singlet oxygen marker genes. Cell death by acute water stress was inhibited by the singlet oxygen scavenger histidine and was accompanied by vacuolar collapse and the appearance of serpin-protease complex. Over-expression of AtSerpin1 also attenuated cell death under this mode of cell stress. Thus, acute water stress damage shows parallels to vacuole-mediated cell death where the generation of singlet oxygen may play a role.

Singlet oxygen is a reactive oxygen species (ROS) that can be produced in a light-dependent manner in the photosynthetic apparatus of plants or can accumulate during certain biochemical reactions. It is a strong electrophile, and can undergo several types of reactions with biological molecules. Of note are cycloaddition reactions on double bonds, forming hydroperoxides via the Alder-Ene reaction, and endoperoxides via the Diels-Alder reaction. It is also able to react with thiols, leading to the production of sulfoxides and sulfinic and sulfonic acids (Triantaphylidès and Havaux, 2009).

Singlet oxygen is a strong oxidant of polyunsaturated fatty acids and is the main source of photooxidative damage in chlorophyll-containing cells in Arabidopsis (Triantaphylidès et al., 2008). The resultant peroxidation reaction initiated by singlet oxygen can create a kink in the hydrophobic fatty acid tail causing irregularities in the membrane ultrastructure and vesicular budding (Riske et al., 2009), or cross linking and aggregation of membrane proteins (Kukreja and Hess, 1992; Beaton et al., 1995). Hence, damage to membrane function by singlet oxygen might arise from two distinct mechanisms: one through a purely physical mechanism of membrane disruption, and the other through failure of membrane pumps that are critical components in the maintenance of homeostasis.

Cellular detoxification of singlet oxygen can be via physical energy transfer or through chemical reactions. The former type involves energy exchange between singlet oxygen and molecules like carotenoids. The latter type of chemical quenching can occur between singlet oxygen and ascorbate, where the quencher is oxidized and consumed. Recycling of the quencher can occur through enzymatic means, such as the ascorbate-glutathione pathway, or via de novo synthesis (Triantaphylidès and Havaux, 2009). Other examples of dissipation occur through specific interaction with amino acids, e.g. Histidine (His) to form endoperoxides (Nilsson et al., 1972; Matheson et al., 1975; Ishibashi et al., 1996).

In addition to direct cytotoxicity, singlet oxygen possesses a signaling function (Kim et al., 2008). For example, in the dark, *FLUORESCENT* (*flu*) mutants accumulate excess protochlorophyllide in the chloroplasts. Protochlorophyllide, a precursor of chlorophyll (Meskauskiene

[1] We acknowledge the support of the I-CORE Program of the Planning and Budgeting Committee and The Israel Science Foundation (grant no. 757/12), the Lerner Family Plant Science Research Fund, and the Israel Science Foundation (grant no. 1596/15).

* Address correspondence to robert.fluhr@weizmann.ac.il.

The author responsible for distribution of materials integral to the findings presented in this article in accordance with the policy described in the Instructions for Authors (www.plantphysiol.org) is: Robert Fluhr (robert.fluhr@weizmann.ac.il).

E.K. formulated the hypotheses and carried out the experimental work and wrote the manuscript; and R.C., A.M., and R.F. formulated the hypotheses and wrote the manuscript.

[OPEN] Articles can be viewed without a subscription.

www.plantphysiol.org/cgi/doi/10.1104/pp.15.02026

et al., 2001), acts as a photosensitizer and generates singlet oxygen, which leads to cell death in Arabidopsis plants when shifted from dark to light conditions (op den Camp et al., 2003). The light-generated cell death and gene induction in *flu* plants depend on *EXECUTER1 and 2*, implying that singlet oxygen plays a signaling role rather than delivering direct toxicity (Wagner et al., 2004; Lee et al., 2007). However, other stresses that stimulate the generation of singlet oxygen in the chloroplast, e.g. high light in the *chlorina 1* mutant, were found to be independent of *EXECUTER* genes and may indicate direct toxicity (Ramel et al., 2013).

Recent work has emphasized light-independent singlet oxygen production in response to wounding or the addition of elicitor in the dark (Mor et al., 2014). Additionally, transcriptome signatures characteristic of singlet oxygen were found to be pervasive in many biotic and abiotic stress conditions. Organelles such as the nucleus, mitochondria, and peroxisome have been reported to be potential sources of singlet oxygen in root tips (Mor et al., 2014). In animal systems, singlet oxygen was shown to be involved in both signaling and membrane photo-oxidation in the cell (Klotz et al., 2003) and in phagocytic immune response (Steinbeck et al., 1992). Hence, the role of singlet oxygen in signaling and cell death is ubiquitous and not restricted to either light dependence or chlorophyll-containing cells.

Plant cell vacuoles are regulators of intracellular and organismal homeostasis and serve as cellular waste recovery stations, where misfolded proteins and damaged organelles are delivered for degradation and disposal. Vacuolar proteases that are important in protein and degradome processing include VACUOLAR PROCESSING ENZYME and RESPONSIVE TO DESSICATION-21 (RD21; Hara-Nishimura et al., 2005; Gu et al., 2012). These proteases can also carry out death-promoting functions in plant programmed cell death (Hatsugai et al., 2004; Kuriyama and Fukuda, 2002; Hara-Nishimura et al., 2005; Lampl et al., 2013). It has been proposed that vacuolar-mediated cell death could proceed by two distinct mechanisms (Hara-Nishimura and Hatsugai, 2011): the destructive pathway, involving disruption of the tonoplast, and a nondestructive pathway, in which the tonoplast membrane remains intact. The nondestructive way is proteasome-dependent, and facilitates the secretion of antipathogenic substances from the vacuole into the apoplast through specific pores. The destructive pathway shares many similar features with necrotic-type programmed cell death pathways in plants such as the hypersensitive response (Hatsugai et al., 2004) and the formation of tracheary elements in xylem development (Kuriyama, 1999).

When the vacuolar membrane is disrupted, e.g. during elicitor-induced vacuolar cell death, proteases like RD21 escape into the cytoplasm, thus exacerbating cell death (Lampl et al., 2013). Its cognate protease inhibitor, AtSerpin1, serves as a potential protective cell death check-point by acting as a suicide substrate, thus inactivating the protease. In one model, when such inhibitors are in excess, cells protect themselves from intracellular damage and survive, but when proteases exceed their inhibitors, the surplus proteases are able to degrade cellular proteins, leading to cell death. Thus, it has been suggested that serpins and proteases exist in a balance governed by their stoichiometric amount and the integrity of compartment membranes (Lampl et al., 2013). Singlet oxygen, if targeted toward membranes of hydrolytic organelles such as the vacuole, could result in the direct disruption of membranes, unleashing their stored proteolytic activity. Here, we demonstrate that singlet oxygen produced in the vacuole, as well as the balance of proteases and their cognate inhibitors, can be components of vacuole-mediated cell death. We further demonstrate that acute water stress in the dark can lead to cell death in a manner that partially mimics singlet oxygen-driven vacuolar-type cell death.

RESULTS

Localization of Photodynamic Singlet Oxygen Generators and Cellular Damage

With the aim of better understanding singlet oxygen toxicity and its possible relationship to vacuole-mediated cell death, we chose to investigate two different photosensitizers, rose bengal (RB) and acridine orange (AO). RB and AO were applied to 5-d-old Arabidopsis seedlings in the dark (Fig. 1A). The plant tonoplast marker *γ-TONOPLAST INTRINSIC PROTEIN* aquaporin fused to the cyan fluorescence protein (CFP) marker was used to assist in determining their localization (Nelson et al., 2007). In the case of RB, staining was observed in the cell periphery, whereas AO was localized to the vacuole. When a hypertonic solution of 1 M mannitol was applied, the vacuole shrunk, revealing RB stain mainly in the plasmalemma (Fig. 1B, top; and Supplemental Fig. S1). When seedlings treated with AO were subjected to the same treatment, the vast majority of AO could be

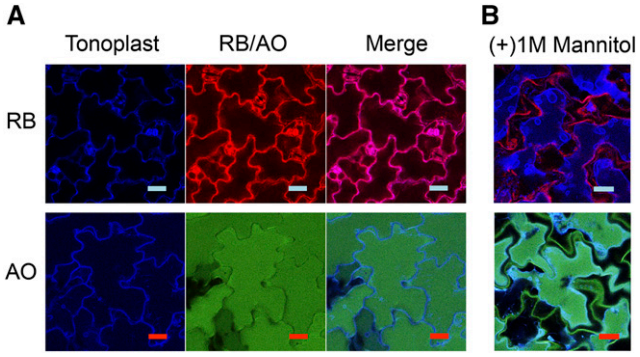

Figure 1. Confocal microscopy of Arabidopsis seedlings showing localization of the photosensitizers RB and AO. A, Recombinant tonoplast marker line (5-d-old; CFP) treated with 100 μM RB (top) and AO (bottom), respectively. B, Seedlings (5-d-old; CFP) treated with 100 μM RB (top) and AO (bottom), respectively, and mounted on a microscope slide with 1 M mannitol to allow for cell plasmolysis. Seedlings were observed by confocal microscopy as described in the "Materials and Methods." Scale bar = 20 μm.

detected within the confines of the vacuole while a residual amount was observed in the cell wall (green color; Fig. 1, A and B, bottom). RB has been shown previously to localize to the cell periphery in Arabidopsis cell cultures and to the chloroplast (Gutiérrez et al., 2014). AO is sequestered in acidic compartments like the vacuole, where it becomes protonated and trapped in the cation form to which the tonoplast membrane is impermeable (Oparka, 1991; Boller and Wiemken, 1986).

Singlet oxygen is among the major reactive oxygen species shown to be involved in chloroplast-based lipid peroxidation in oxidative-type cell death, e.g. in high light stress (Triantaphylidès et al., 2008). It is therefore of interest to examine the ramifications of its accumulation in other cellular compartments. Both AO- and RB-treated plants showed light-dependent cell death as determined by ion leakage (Fig. 2A). The kinetics of the cell death profiles of the two photosensitizers appear to be different. RB treatment induced rapid light-dependent ion leakage as early as 2 h but decelerated cell death toward the later time points (Fig. 2B). In contrast, AO-treated samples showed a delayed cell death profile, which started to accelerate after 24 h (Fig. 2C).

His scavenges singlet oxygen and hydroxyl radicals with a high degree of specificity by both physical and chemical mechanisms (Nilsson et al., 1972; Matheson et al., 1975; Ishibashi et al., 1996). His effectively scavenged RB-induced singlet oxygen production in vitro as shown by measuring the changes in fluorescence of the singlet oxygen sensor green (SOSG) probe, after light treatment (Supplemental Fig. S2). We tested the scavenging effect of His against both RB- and AO-generated phototoxicity in vivo. AO-photosensitized cell death was reduced by His (Fig. 2E). However, RB-treated samples showed an unexpected increase in apparent cell death in the presence of His (Fig. 2D). Photo-oxidized His forms reactive endoperoxide intermediates (Cadet and Di Mascio, 2006) that can be toxic. Apparently, the local cellular milieu can impact on the efficacy of His to act as a protective scavenger.

AO But Not RB Induces Vacuolar Destruction

Cell death rates approaching 40% were observed after 72 h light treatment in both RB and AO applications (Fig. 2, B and C). A residual fluorescent signal from AO was evident after 72 h in the light and dark that differed from the initial distribution (compare Figs. 1A and 3A). In addition, in the light the vacuolar membrane marker was disrupted (Fig. 3A, compare light and dark). Additional CFP fluorescent material of unknown origin also appears to accumulate in the vacuole after extended 72 h of AO treatment in the dark (Fig. 3A). In contrast, in RB-treated tissue after 72 h, the residual fluorescent signal was mostly bleached in the light but the vacuolar membrane appeared intact (Fig. 3B, compare light and dark). Sytox-Green staining was used to examine the integrity of membranes in RB treatments. Sytox Green enters cells with compromised plasmalemma and binds to nucleic acids. Sytox-Green staining of RB-treated tissue showed that the cell outer membrane was rendered permeable by RB phototoxicity in the light but not in the dark, with little effect on the tonoplast structure (Supplemental Fig. S3, compare light and dark). Thus, photodynamic cell death with RB and AO showed distinctive kinetics of ion leakage and differential effect of the photodynamic process on the tonoplast membrane, suggesting distinct mechanisms of cell death.

AO But Not RB Induces Mixing of Cytoplasm and Vacuolar Compartments

The ablation of the tonoplast membrane by AO treatment in the light suggested the possibility that application of AO could mimic vacuolar-mediated cell

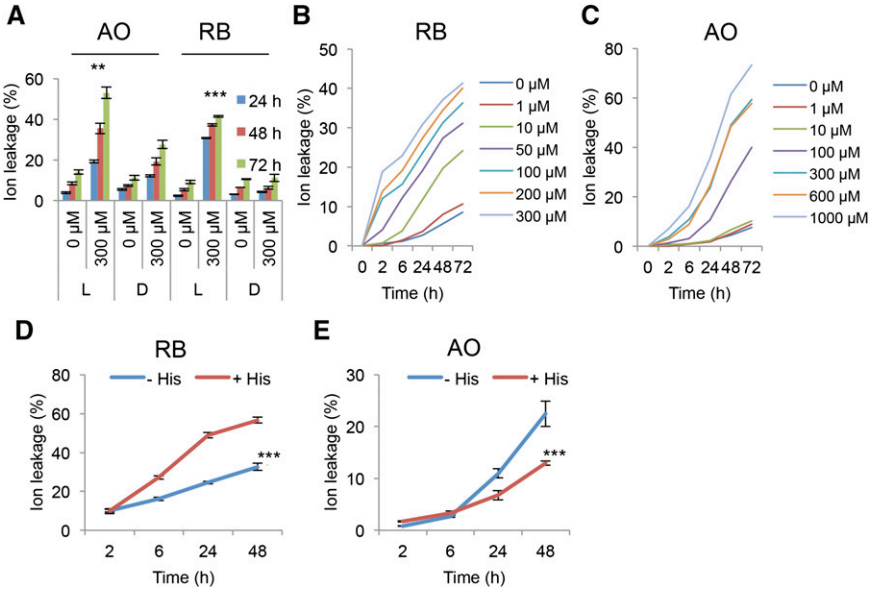

Figure 2. Ion leakage in Arabidopsis plants showing effects of photosensitizers AO and RB in the light and dark. A, Ion leakage assay. Leaf discs were treated with 300 μM AO and RB, respectively, and incubated for 0, 24, 48, and 72 h in the light (L) or dark (D). Student's *t*-test was performed for similar concentrations between light/dark for each individual group (**, $P < 0.01$; ***, $P < 0.001$). B, C, Kinetics of ion leakage. Leaf discs were treated with different concentrations of RB (B) and AO (C) for 0, 24, 48, and 72 h in the light. D and E, His protection assay. Arabidopsis leaf discs were incubated with 100 μM RB (D) or AO (E) in the presence or absence of 10 mM His, and measured at 0, 2, 6, 24, and 48 h. Means and SE are presented. The data were analyzed using repeated measures two-way ANOVA (***, $P <$ 0.001).

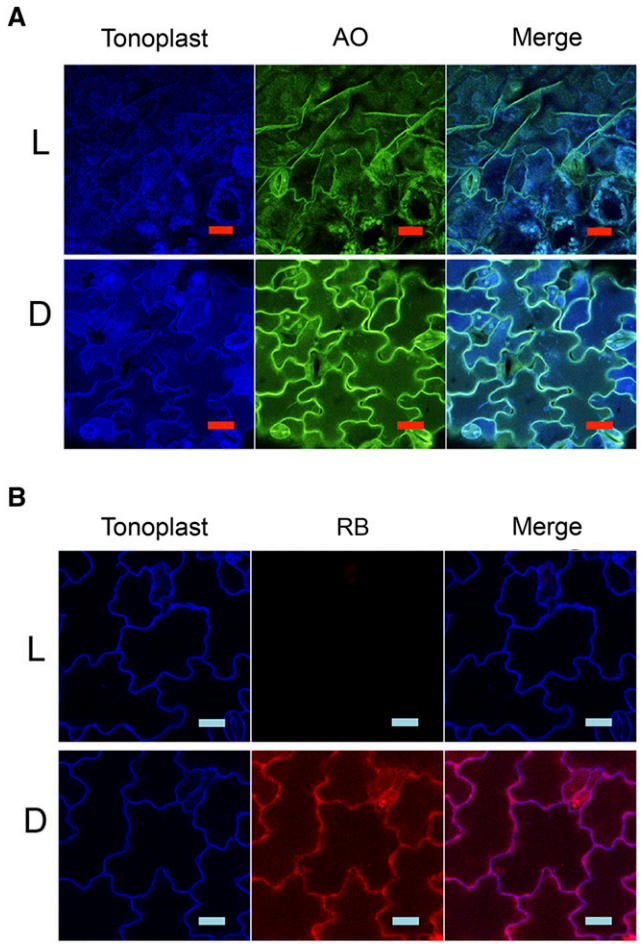

Figure 3. Confocal microscopy of Arabidopsis seedlings treated with photosensitizers AO and RB in the light (L) and the dark (D). Seedlings (5 d old, with tonoplast marker) were treated with 100 μM of AO (A) or RB (B) and incubated for 72 h in the light or dark and mounted on a microscope slide for observation by confocal microscopy. Scale bar = 20 μm.

death that is characterized by the mixing of cytoplasmic and vacuolar contents. To visualize this at the molecular level, we took advantage of the fact that the AtSerpin1-HA protease inhibitor is expressed in the cytoplasm and can form a covalent complex with the vacuolar RD21 protease upon mixing of cellular compartments (Lampl et al., 2010). Photodynamic cell death was induced in an AtSerpin1-HA over-expression line by treating plants with or without 100 μM RB or AO under continuous light conditions. Extracts were treated with Cys protease inhibitor E-64 to prevent further formation of complex (Roberts et al., 2011) and fractionated on nonreducing sodium dodecyl sulfate-polyacrylamide-gel electrophoresis (SDS-PAGE) gel (Fig. 4). Inspection of the Coomassie-stained gel shows a gradual decrease in the levels of the large subunit of RUBISCO (Rubisco) that is accelerated in AO and RB. The decrease in Rubisco may indicate a more rapid turnover of cellular proteins due to cell death over 72 h. Immunoblots were developed with AtSerpin1 antibody to detect serpin-protease complex. Significantly more complex accumulated in the samples treated by AO compared to the control with concomitant disappearance of the free serpin at 45 kD. The increased appearance of cleaved spent serpin likely represents turnover of complex that frees the residual N-terminal (37 kD) fragment. An additional higher M_r immune-reactive polypeptide was present in AO-treated samples in the light and the dark (Fig. 4; Supplemental Fig. S4). This may be due to the presence of an additional AO-induced serpin-protease complex. The presence of additional serpin-protease complexes has been noted before (Lampl et al., 2010). The presence of this putative higher M_r complex in the dark and the light indicates that it is likely not due to the production of singlet oxygen. In the RB-treated sample, no complex or free serpin were detected although spent serpin was observed. Spent serpin can result from disassociation of complex or activation of noncognate proteases that cleave the serpin (Lampl et al., 2010). In the dark, control, AO and RB treatments are similar except for the presence of the higher M_r immune-reactive polypeptide in the AO-treated sample mentioned above (Supplemental Fig. S4). All samples showed a gradual accumulation of complex but to a lesser extent than observed in the light with AO, and may be a result of autophagic cellular processes that utilize RD21 protease and are stimulated under dark starvation conditions. Taken together, the enhanced formation of complex implies that AO photodynamic damage led to mixing of cytoplasmic and vacuolar contents. In contrast, the photodynamic activity of RB led to cell death without apparent vacuolar collapse or mixing of compartments.

AtSerpin1 in the Cytoplasm Can Partially Protect Cells from Vacuolar-Mediated Cell Death

Serpins are localized to the cytoplasm and are thought to serve a cytoprotective function from vacuolar cell

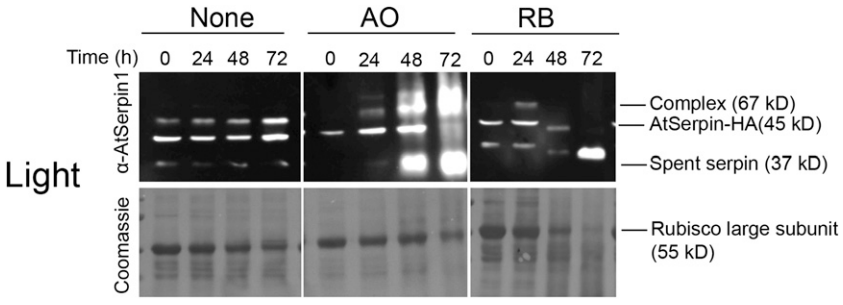

Figure 4. Immunoblots of photosensitizer-treated samples. Arabidopsis leaf discs from AtSerpin1 over-expression (HA) lines were treated with 100 μM AO or RB or mock-treated (None) and incubated in the light for 0, 24, 48, and 72 h. Extracts were treated with 50 μM E64 and fractionated on nonreducing SDS-PAGE and developed with α-AtSerpin1 antibody. The bottom images show the corresponding Coomassie staining.

death proteases (Lampl et al., 2013). We asked if photodynamic cell death could bring about the release of vacuolar proteases that would be impacted by the presence of serpins in the cytoplasm. To this end, the response of wild-type, over-expression AtSerpin1-HA (HA), AtSerpin1 knockout (AtSerpin1-ko), and RD21 knockout (RD21-ko) plant lines were analyzed (Fig. 5). AtSerpin1-HA lines showed a protective effect to photodynamic-mediated damage after AO treatment (Fig. 5B, P-value < 0.001). The RD21-ko lines were less effective in the reduction of cell death (P-value < 0.057), while the AtSerpin-ko lines were not statistically different from the wild-type lines. This may be due to gene redundancy. Under dark conditions no statistical difference can be measured between any of the lines (Supplemental Fig. S5). Significantly, none of the RB-treated plant lines showed differences from each other in the light (Fig. 5A). This indicates that the serpin-protease system does not play a role in RB-motivated cell death and is consistent with the lack of formation of serpin-protease complex (Fig. 4). Taken together, the results suggest that serpin over-expression or the absence of RD21 protease can mitigate vacuolar-type cell death. It is possible that the presence of multiple proteases in the vacuole explain why only partial protection was afforded by RD21-ko and AtSerpin1-HA lines.

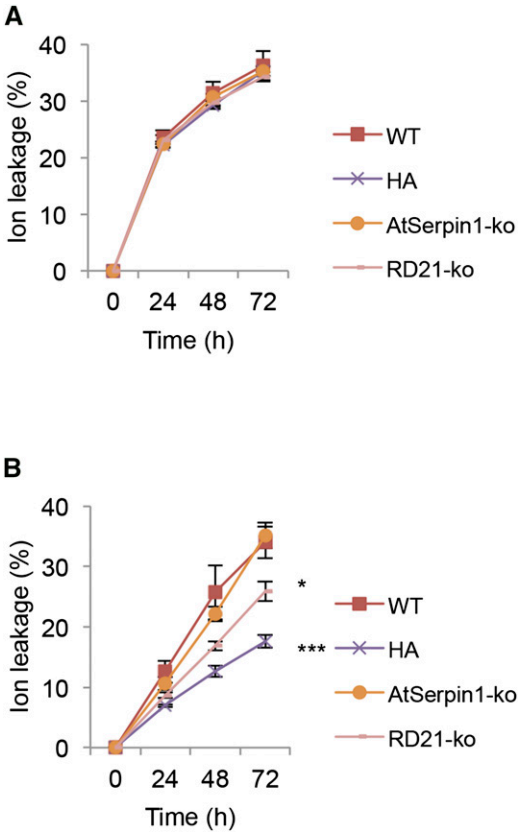

Figure 5. Ion leakage assay of various Arabidopsis mutant lines treated with RB and AO. Arabidopsis leaf discs were treated with 100 μM of RB (A) or AO (B) and incubated in the light for 0, 24, 48, and 72 h. Lines used were wild type; AtSerpin1 over-expression line (HA); AtSerpin1 insertion mutant (AtSerpin1-ko); and RD21 insertion mutant (RD21-ko). The experiment was repeated three times, with means and SE presented. Data were analyzed by repeated-measures two-way ANOVA. Significance established by pairwise comparisons to the wild-type line using a post hoc Dunnett test (*, $P < 0.05$; ***, $P < 0.001$).

Dehydration Treatment in the Dark Produces Singlet Oxygen and Vacuolar Disruption

Transcriptomic signatures for singlet oxygen appear in many diverse stresses including water stress (Mor et al., 2014). It is therefore of interest to compare tissue death induced by this stress with photodynamic-induced cell death. Leaf tissue was dehydrated for various times (1–3 h) and then analyzed over 72 h. Dehydration treatments of 2 and 3 h led to 20% and 60% cell death, respectively, after 72 h. Cell death was rapid and reached a plateau 2 h after treatment (Fig. 6A). The application of His decreased damage by dehydration, as measured by a reduction in ion leakage by more than 30% (Fig. 6C, $P < 0.01$). To further substantiate a possible role for singlet oxygen in this type of tissue death, Arabidopsis seedlings were dehydrated in the dark and treated with the highly specific SOSG probe that forms diagnostic endoperoxides in the presence of singlet oxygen (Flors et al., 2006). A rise of fluorescence, indicating singlet oxygen-dependent formation of endoperoxide, was detected rapidly in the cytoplasm after 15 min of dehydration (Fig. 6B). After 30 min of drying treatment in the dark, the SOSG reporter was observed to permeate the cell. In contrast, in wet control samples placed in the dark for similar times, no SOSG fluorescence was detected and the tonoplast remained intact (Supplemental Fig. S6).

To quantitate singlet oxygen production, the spin trap, 4-hydroxy-TEMP (4-hydroxy-tetramethylpiperidine), was employed. It shows enhanced specificity for singlet oxygen that can be detected by electron paramagnetic resonance spectroscopy (EPR; Nakamura et al., 2011). EPR spectra obtained from RB- and dehydration-treated plants indicate a comparable production of singlet oxygen. However, in AO-treated plants a reliable spectrum was not observed (Fig. 6D, Supplemental Fig. S7). AO treatment may generate a signal that is too low for detection or the singlet oxygen is sequestered from the spin-trap probe. As singlet oxygen will react with membrane lipids to form hydroperoxyl lipid radicals and lipid peroxidation, these products can be detected by the thiobarbituric acid-reactive substances (TBARS) assay (Hodges et al., 1999). As shown in Fig. 7, RB, AO, and dehydration treatments led to the detection of statistically significant increases in TBARS equivalents. Taken together, the evidence from SOSG fluorescence, 4-hydroxy-TEMP oxidation, and the detection of lipid peroxidation products by TBARS is consistent with singlet oxygen production leading to a degree of lipid peroxidation.

The rapid permeation of the vacuole by SOSG may indicate a contribution of vacuolar collapse to dehydration-induced cell death. To examine this, tonoplast integrity was followed by serpin-protease complex formation. The

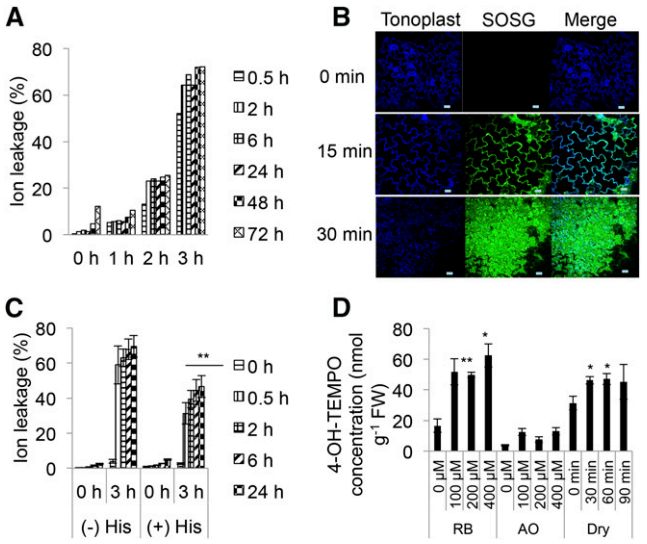

Figure 6. Ion leakage and singlet oxygen production during RB, AO, and acute water treatments. A, Ion leakage assay. Leaf discs from 10-week-old wild-type (Col-0) plants were subjected to various dehydration treatments for 0, 1, 2, and 3 h and then rehydrated and incubated under continuous light (30 μE). Readings were taken at 0, 0.5, 2, 6, 24, 48, and 72 h. B, Confocal imaging of Arabidopsis seedlings subjected to dehydration. Seedlings with the tonoplast marker (5 d old) were subjected to dehydration for 0, 15, 30 min, and incubated with 100 μM SOSG in the dark, and mounted on a microscope slide for observation by confocal microscopy as described in the "Materials and Methods". Scale bar = 20 μm. C, Ion leakage assay. Leaf discs were preincubated with 10 mM His, subjected to dehydration treatment (0 and 3 h), and incubated under continuous light (30 μE). Readings were taken at 0, 2, 6, and 24 h. The experiment was repeated twice, with means and SE presented. The data were analyzed using repeated-measures two-way ANOVA (**, $P < 0.01$). D, EPR of RB-, AO-, and dehydration-treated seedlings. Wild-type seedlings were incubated with 0.4 M 4-hydroxy-TEMP containing 0, 100, 200, and 400 μM RB or AO in the dark for 30 min, washed, and incubated in the light (30 μE) for 2 h. For dehydration, wild-type Arabidopsis seedlings were incubated with 0.4 M 4-hydroxy-TEMP for 30 min, washed, and then placed on dry Whatman paper for 0, 30, 60, and 90 min in the dark. Extraction was performed as described in the "Materials and Methods" before analysis by EPR spectroscopy. The means and SE of three replicates is shown. Analyses by two-way ANOVA, followed by a post hoc Tukey test, or a Student's *t*-test was performed against their respective controls for significance (*, $P < 0.05$; **, $P < 0.01$).

amount of AtSerpin1-protease complex and spent cleaved serpin increased as a result of dehydration stress in mature plants (Fig. 8A) or in seedlings (Supplemental Figs. S8 and S9). This observation indicates a degree of mixing of cellular compartments due to dehydration stress but to a lower degree than observed for AO treatment. To test this observation further, wild-type, over-expression AtSerpin-HA, AtSerpin1-ko, and RD21-ko were examined for their sensitivity to drought simulation. In this case, only a small but statistically significant reduction (Fig. 8B; 18%; $P < 0.05$) in ion leakage was noted in the over-expression AtSerpin1-HA line. Taken together, the results indicate that acute water stress induced a degree of permeabilization of the vacuolar membrane as indicated by the distribution of SOSG fluorescence, disruption of the CFP tonoplast marker, and by the formation of serpin-protease complex.

Gene Expression Markers for Singlet Oxygen

To further characterize the types of ROS produced under photodynamic and dehydration stress, quantitative real-time PCR analysis was carried out with gene sets specific for types of ROS. Singlet oxygen was shown to induce gene sets At3g61190, At5g64870, and At3g01830 whereas superoxide/hydrogen peroxide induced At5g01600, At4g21870, and At1g71030 (op den Camp et al., 2003). As expected, RB and AO showed specific induction of the singlet oxygen probes, while methyl viologen (MV) preferentially induced the expression of the superoxide/hydrogen peroxide probes (Fig. 9A). The strength of gene induction by AO appears to be less than RB, a result that is consistent with its reduced quantitative EPR and TBARS measurements. Strikingly, the gene induction pattern of dehydration treatment is robust, and closely follows that of singlet oxygen (Fig. 9B).

DISCUSSION

Singlet oxygen generators that localized to the plasma membrane and vacuole, respectively, generate very different patterns of cell death. RB accumulated in the cell periphery and stimulated rapid ion leakage. The permeabilization of the plasmalemma by RB treatment left the tonoplast intact, as evidenced by the entry of Sytox Green, but the integrity of the tonoplast marker was maintained. RB also generated singlet oxygen that was measurable by singlet oxygen spin traps as well as by lipid peroxidation, established by TBARS assay. In contrast, AO was sequestered in the vacuole and stimulated slower ion leakage without detectable

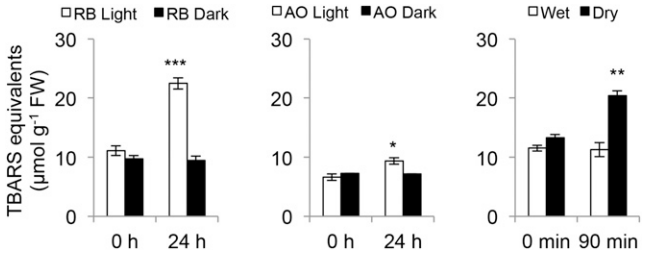

Figure 7. TBARS assay of RB, AO, and dehydration-treated Arabidopsis. Wild-type Arabidopsis seedlings were incubated with 100 μM of RB or AO for 1 h in the dark, then washed and incubated in the light (30 μE) or dark for 0, 24 h. Dehydration treatment was performed on wild-type Arabidopsis seedlings on dry Whatman paper or in water in the dark for 0, 90 min. The TBARS assay was performed as described in the "Materials and Methods". The means and SE of three replicates is shown. Student's *t*-test of the different concentrations of RB or AO was performed against their respective controls for significance (*, $P < 0.05$; **, $P < 0.01$).

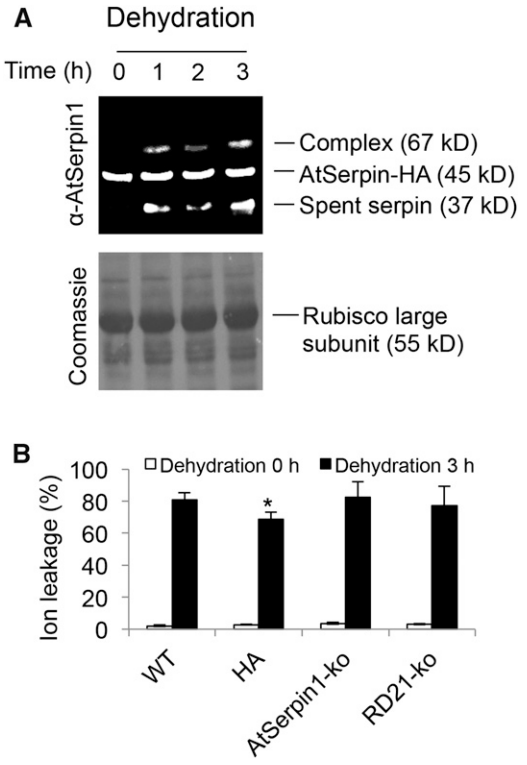

Figure 8. Arabidopsis mutant lines treated by dehydration stress. A, Immunoblot of dehydration-treated plant AtSerpin1-HA. Leaf discs were treated on dry blotting paper for 0–3 h as indicated, replaced in ddH_2O for 1 h before harvesting. Extracts were treated with 50 μM E64 and fractionated on nonreducing SDS-PAGE and developed with α-AtSerpin1 antibody. The bottom image shows the corresponding Coomassie staining. B, Ion leakage assay. Leaf discs from mutant plant lines as in Figure 5 were subjected to 3 h dehydration treatment. Ion conductance readings were taken at 0 and 24 h. The experiment was repeated two times with means and SE presented. Student's *t*-test of each line against the wild-type line was performed for significance (*, $P < 0.05$).

singlet oxygen production by EPR. Trivially, one may suspect that no singlet oxygen was made; however, this is inconsistent with the detection of lipid peroxidation by the TBARS assay and the finding that both treatments resulted in the induction of singlet oxygen specific genes. The discrepancy can be reconciled by noting that AO-generated singlet oxygen is less amenable to detection by spin-trap probes (Ito, 1978; Decuyper et al., 1984). In addition, the vacuole may be less accessible to the spin-trap probe.

AO treatment was characterized by extensive tonoplast collapse and the release of vacuolar cell death proteases that could be followed by formation of serpin-protease complexes. This occurred even though the amount of singlet oxygen produced by AO is low, indicating that the vacuolar membrane is sensitive to this level of singlet oxygen. When the vacuole membrane is ruptured and the amount of released protease exceeds the capacity of the serpin, the subsequent widespread proteolysis of intracellular proteins disrupts cellular homeostasis (Yamashima, 2004). This stimulates a positive feedback loop that spirals to cell death that can be partially reversed in AtSerpin1 overexpression lines due to formation of inactive serpin-protease complexes. Significantly, photodynamic cell death as rendered by AO shows a degree of commonality with vacuolar-mediated programmed cell death as described for certain plant-pathogen interactions (Hara-Nishimura and Hatsugai, 2011; Dickman and Fluhr 2013).

In an analogous manner, AO applied to malignant melanoma cells was shown to accumulate in cellular acidic compartments that were disrupted in a photodynamic process that led to cell death (Hiruma et al., 2007). Death by RB is different and is likely through plasmalemma membrane permeabilization that initiates rapid ion leakage. Indeed, cercosporin, a lipophilic singlet oxygen generator secreted by necrotrophic phytopathogens of the *Cercospora* species is thought to accumulate in the membranes of host cells (Daub and Briggs, 1983; Daub and Ehrenshaft, 2000). Rapid electrolytic leakage was detected from a variety of plant leaf discs treated with cercosporin within minutes of exposure to light (Daub and Briggs, 1983; Macri and Vianello, 1979). Thus, RB and AO initiate qualitatively

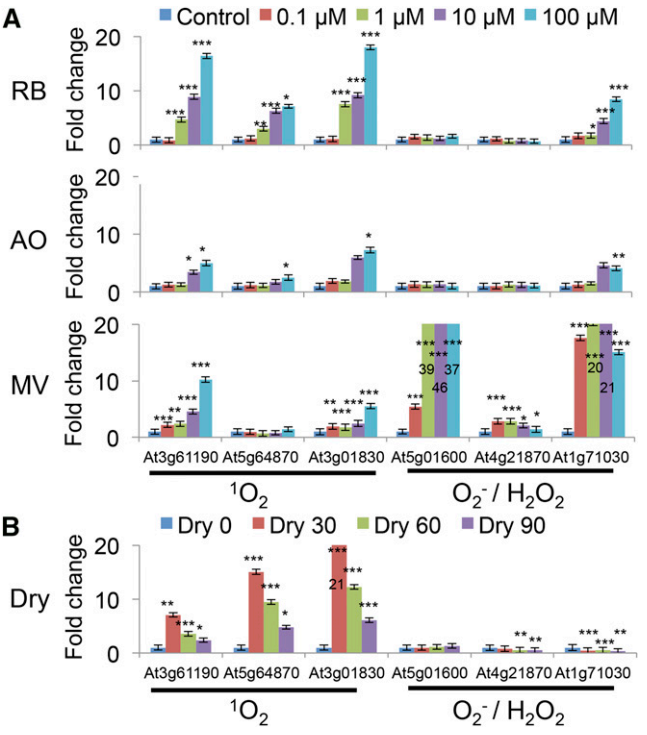

Figure 9. Quantitative real-time PCR using $^1O_2$- and O_2^-/H_2O_2-sensitive genes under various treatments. A, Seedlings were incubated with 0, 0.1, 10, and 100 μM of RB, AO, and MV in the dark for 1 h, washed and then incubated in the light (30 μE) for 2 h. B, Seedlings were subject to 0, 30, 60, and 90 min of dehydration in the dark. In MV treatment, numbers in column represent off-the-scale values. The means and SE of three replicates is shown. Student's *t*-test was performed against their respective controls for significance (*, $P < 0.05$; **, $P < 0.01$; ***, $P < 0.001$).

different pathways of cell death and each partially mimics distinct physiological situations.

The role of singlet oxygen in promoting cell death is an open question. The direct oxidative action of singlet oxygen, especially on lipids and membrane-bound proteins suggests that singlet oxygen can exert its toxicity through modulating membrane integrity (Riske et al., 2009; Kukreja and Hess; 1992; Beaton et al., 1995). Alternatively, singlet oxygen produced by the *flu* mutant in the chloroplast has been shown to induce cell death through signaling components rather than by direct toxicity. The expression of *flu*-induced stress genes requires the genes *EXECUTER1&2* (Wagner et al., 2004; Lee et al., 2007; Kim et al., 2012; Kim and Apel, 2013). Additionally, under high light stress the photodynamic overflow caused by singlet oxygen circumvents the *EXECUTER1&2* signaling pathway to directly induce cell death (Kim et al., 2012).

Dehydration stress was shown here to directly involve singlet oxygen accumulation based on SOSG fluorescence and EPR measurements. These observations are consistent with attenuation of cell death by the scavenger His and by induction of singlet oxygen-specific genes. While tonoplast disruption was prominent during acute water stress, the formation of serpin-protease complex and protection by AtSerpin1 over-expression was less robust compared to photodynamic vacuolar destruction using AO. This may be due to the rapidity of death or alternatively, acute water stress cell death may induce a conglomerate of destructive forces of which vacuolar integrity is but one layer.

It is thought that drought accelerates cell death through photooxidative stress. In one mechanism, stomatal closure that limits water loss also restricts CO_2 intake, leading to a reduction of the net photosynthetic rate that causes the overall generation of ROS (Mittler, 2002; Cruz de Carvalho, 2008). The main ROS that are produced in this fashion are O_2^-, H_2O_2, and singlet oxygen through the over-reduction of the light harvesting photosystems and photorespiration (Cruz de Carvalho, 2008; Krieger-Liszkay et al., 2008). However, as shown here, and previously for root tissue (Mor et al.., 2014), drying of plant tissue in the dark also leads to ROS production in the form of singlet oxygen.

The source of singlet oxygen in driving chloroplast-induced cell death in the light is chlorophyll. The source of singlet oxygen in the dark is unknown. Singlet oxygen has a short half-life implying that its production is cell autonomous. Also, the presence of singlet oxygen in the dark in the cytoplasm of leaf epithelial cells that are largely devoid of chloroplasts indicate that chlorophyll is not a source. Evidence was recently presented for singlet oxygen production in other organelles such as the mitochondria, peroxisomes, and in general in membrane-rich regions (Mor et al., 2014). Singlet oxygen could arise in the dark by reaction of O_2^- and H_2O_2 via the Haber-Weiss reaction (Khan and Kasha, 1994). For example, singlet oxygen lipid peroxidation signatures were present when MV, which is an inducer of O_2^- and H_2O_2, was applied to Arabidopsis leaf discs (Triantaphylidès et al., 2008). However, the results here show that acute water stress induces marker genes related to singlet oxygen rather than O_2^- or H_2O_2. Singlet oxygen could also arise through the Russell mechanism in the chemical reactions produced by peroxylipid radicals that are initiated by lipoxygenase activity (Kanofsky and Axelrod, 1986; Miyamoto et al., 2007). Indeed, drought-activated increases in lipoxygenases were detected in Arabidopsis leaves (Gigon et al., 2004), and roots (Grebner et al., 2013). A ubiquitous stress signaling mechanism for activation of lipoxygenases may involve cellular calcium. Calcium is rapidly elevated during drought stress (Knight et al., 1997), and was shown to activate both lipoxygenase activity (Nelson et al., 1997) and the general quasi-lipoxygenase activity of hemoproteins (Iwase et al., 1998). It will be of interest to see how singlet oxygen integrates into the temporal sequence of events from stress to ROS generation to changes in gene expression (Laloi and Havaux, 2015; Dietz, 2014).

Production of singlet oxygen that is independent of light and chloroplasts appears to be a common component in vacuolar cell death. Whether singlet oxygen directly causes membrane permeabilization, or by working through some other means, remains to be elucidated. Singlet oxygen transcriptome signatures are also manifest in other abiotic and biotic stresses (Mor et al., 2014). Hence, it would be important to characterize the role of singlet oxygen in these stresses, and examine if there are similarities between the resulting types of cell death.

MATERIALS AND METHODS

Plant Growth Conditions and Treatments

Arabidopsis thaliana (ecotype Columbia-0) seedlings (5 d to 3 weeks) were grown under white light in a 16 h light/8 h dark cycle at 21°C on Murashige and Skoog medium, supplemented with 1% Suc and 0.8% (w/v) phytoagar (Invitrogen, Carlsbad, CA). Arabidopsis plants (8–12 weeks) were grown in soil under a 12 h light/dark cycle at 21°C. All the in vivo experiments treated with rose bengal (RB) and acridine orange (AO) were supplemented with 1% Suc, while all the dehydration experiments were performed in ddH_2O. For the in vitro singlet oxygen assay 10 μM of RB (Sigma) and 1 μM of singlet oxygen sensor green probe (SOSG; Sigma) were prepared in ddH_2O and fluorescence measured at 485 nm excitation and 525 nm emission after exposing to white light (30 μE) for 5 min intervals over 45 min.

Cell Death Assays with Ion Leakage

Ion leakage was performed on ten 5-d-old seedlings or five leaf discs (6 mm; 8–12 weeks) per well in a 12-well plate (Corning Life Sciences, Corning, NY) in 5 mL of ddH_2O or 1% Suc as stated, with three biological replicates for each treatment. The samples were equilibrated in the light for 1 h, and solutions replaced. Following this step, if photosensitizers (RB and AO) were used, incubation was performed in the dark for 1 h, followed by three washes. For drought treatment, leaf discs, or seedlings were placed on dry Whatman paper in the dark for time lengths as stated. Ion conductance was measured by sampling 100 μL using a model no. B-173 Compact Conductivity Meter (Horiba, Kyoto, Japan). If His was used, solutions were made in ddH_2O or 1% Suc as stated, adjusted to pH 7.2, and added after the wash step but before baseline measurement. Samples were incubated under white light (30 μE) or in the dark (wrapped in aluminum foil) as indicated. Maximum ion leakage was obtained after boiling the samples in the microwave for 30 s, followed by another 15 s of boiling, and then cooling at room temperature for 2 h. Relative cell death was calculated by subtracting the baseline and obtaining the ratio over the maximum ion leakage. Means and SES were obtained thereafter.

Immunoblots

Extraction of proteins and their fractionation on reducing and nonreducing denaturing gels has been described in Roberts et al., (2011). Membranes were developed with anti-AtSerpin1 antibodies (1:1000) and secondary anti-guinea pig horseradish peroxidase (1:3000) or with anti-RESPONSIVE TO DESSICATION-21 antibodies (1:1000), and secondary anti-mouse horseradish peroxidase (1:3000).

Confocal Microscopy

Confocal microscopy analysis was carried out on 5–8-d-old tonoplast-labeled cyan-fluorescence-protein marker line (vac-ck CS16256; Nelson, et al., 2007). All images were taken with either a model no. IX81 FV1000D Spectral Type (Olympus, Melville, NY) or a model no. A1 Confocal Microscope (Nikon, Melville, NY). For CFP, excitation was at 405 nm using an argon laser and emission was at 440 nm. SOSG staining was performed by incubation with 100 μM SOSG diluted in ddH_2O in the dark for 20 mins. Sytox-Green staining was performed by incubation with 250 nM Sytox Green diluted in ddH_2O in the dark for 20 mins. For staining by Sytox Green, Singlet Oxygen Sensor Green (SOSG, Invitrogen), and AO, excitation was at 488 nm and emission was at 525 nm. For RB staining, excitation was at 561 nm and emission was at 580 nm. The various photosensitizer and drought treatments were performed on 5–8-d-old transgenic stable marker lines. Seedlings were equilibrated in ddH_2O or 1% Suc as stated for 1 h in the light, and solutions replaced. Following this step, if photosensitizers (RB and AO) were used, incubation was performed in the dark for 1 h, followed by three wash steps, and exposed to light for the time lengths stated. For drought treatment, seedlings were placed on dry Whatman paper in the dark for time lengths as stated, and stained with SOSG as indicated.

RNA Extraction and Quantitative Real-Time PCR Analysis

Arabidopsis seedlings (2-weeks-old, seven seedlings per biological replicate, three replicates) were used for each treatment. RNA was extracted from frozen tissues using a standard Trizol extraction method (Sigma-Aldrich, St. Louis, MO). DNase I (Sigma-Aldrich)-treated RNA was reverse-transcribed using a high-capacity cDNA reverse transcription kit according to the manufacturer's instructions (Quanta Biosciences, Gaithersburg, MD). For quantitative real-time PCR (qRT-PCR) analysis, the SYBR Green method (Kapa Biosystems, Wilmington, MA) was used on a Step One Plus platform (Applied Biosystems, Foster City, CA) with a standard fast program. qRT-PCR primers were designed in SnapGene software (http://www.snapgene.com/). All qRT-PCR primer sequences are listed in Supplemental Table S1.

Electron Paramagnetic Resonance Spectroscopy and Sample Preparation

Arabidopsis seedlings (30 seedlings, 2-week-old) were used for each treatment. The seedlings were equilibrated in ddH_2O for dehydration or 1% Suc for AO and RB in ambient light for 2 h, replacing the medium after 1 h. All further incubation and extraction procedures were carried out in the dark. For dehydration treatment, seedlings were incubated with 0.4 M of 4-hydroxy-TEMP (2,2,6,6-Tetramethyl-4-piperidinol, Sigma-Aldrich) for 30 min, and washed six times with ddH_2O. Samples were then placed on dry Whatman paper for 0, 30, 60, 90 min. Wet samples were floated in a petri dish with ddH_2O for similar times as a control. For RB and AO treatments, 100 μM of RB or AO was coincubated with 0.4 M 4-hydroxy-TEMP prepared in 1% Suc for 30 min, washed, and placed in the light (30 μE) or dark for 2 h. Samples were harvested by flash-freezing in liquid nitrogen and were homogenized in a shaker using glass beads. The samples were then dissolved in 1 mL of 0.2 M potassium-P buffer, pH 7.4, containing 10 mM EDTA and 20 mM N-ethyl-maleimide, and then incubated in a rotator for 15 min at 4°C. The extracts were then centrifuged at 14,000 rpm at 4°C for 20 min, and the supernatant was used for the electron paramagnetic resonance (EPR) measurements. EPR measurements were acquired at room temperature with a model no. ELEXYS E500 Spectrometer (Bruker, Billerica, MA) operating at X-band frequencies (9.5 GHz) and a 100 kHz modulation frequency. The spectra exhibit a typical TEMPO triplet EPR spectra (a_N = 15.8 G) and signal intensity values of the third peak of the nitroxide spectrum were obtained by calculating the difference between the maximum and minimum points, and normalized to the wet weight of the sample and the volume of extraction buffer used. Measurements of 4-hydroxy-TEMPO production induced by singlet oxygen were calculated by plotting against a standard curve of 4-hydroxy-TEMPO.

Thiobarbituric Acid-Reactive Substances Assay

Arabidopsis seedlings (2-week-old, five seedlings per biological replicate, with three replicates) were used for each treatment. The seedlings were equilibrated in distilled, deionized water (ddH_2O) or 1% Suc in ambient light for 2 h, replacing the medium with fresh ddH_2O or 1% Suc after 1 h. For RB and AO treatments, samples were incubated in the dark with 100 μM RB or AO in 1% Suc for 1 h, washed, and then incubated in the light (30 μE) or dark for various time points as stated. For dehydration treatment, samples were incubated on dry Whatman paper or ddH_2O in the dark for the various time points stated. Samples were harvested by flash-freezing in liquid nitrogen and were homogenized in a shaker using glass beads. The TBARS assay was performed according to the method of Hodges et al., (1999). The samples were preweighed before treatment, and TBARS values were normalized according to the wet weights.

Supplemental Data

The following supplemental materials are available.

Supplemental Figure S1. Treatment of RB and AO stained recombinant tonoplast marker line with hyperosmotic concentrations of mannitol.

Supplemental Figure S2. In vitro assay showing scavenging of Rose Bengal generated singlet oxygen by histidine.

Supplemental Figure S3. Confocal microscopy of Arabidopsis seedlings showing RB-induced permeabilization of cell membrane.

Supplemental Figure S4. Immunoblots of photosensitizer treated samples in the dark.

Supplemental Figure S5. Ion leakage assay of various Arabidopsis plant lines treated with RB and AO.

Supplemental Figure S6. Confocal imaging of Arabidopsis seedlings in the dark as a control for dehydration treatment (Figure 6B).

Supplemental Figure S7. Representative EPR spectra of samples from Figure 6D.

Supplemental Figure S8. Arabidopsis plants under dehydration treatment.

Supplemental Figure S9. Immunoblots of dehydration treated plant lines.

Supplemental Table S1. Primers used for qRT-PCR.

Received January 4, 2016; accepted February 12, 2016; published February 16, 2016.

LITERATURE CITED

Beaton S, McPherson RA, Tilley L (1995) Alterations in erythrocyte band 3 organization induced by the photosensitizer, hematoporphyrin derivative. Photochem Photobiol **62:** 353–355

Boller T, Wiemken A (1986) Dynamics of vacuolar compartmentation. Annu Rev Plant Physiol **37:** 137–164

Cadet J, Di Mascio P (2006) Peroxides in biological systems. *In* Z. Rappoport, ed, Patai Series: The Chemistry of Functional Groups. The Chemistry of Peroxides, **Vol. 2**. Wiley, New York. 915–1000

Cruz de Carvalho MH (2008) Drought stress and reactive oxygen species: production, scavenging and signaling. Plant Signal Behav **3:** 156–165

Daub ME, Briggs SP (1983) Changes in tobacco cell membrane composition and structure caused by cercosporin. Plant Physiol **71:** 763–766

Daub ME, Ehrenshaft M (2000) The photoactivated *Cercospora* toxin cercosporin: Contributions to plant disease and fundamental biology. Annu Rev Phytopathol **38:** 461–490

Decuyper J, Houba-Hein N, Calberg-Bacq CM, Van de Vorst A (1984) Evidence for the production of singlet oxygen by photoexcited acridine orange. Photochem Photobiol **40:** 149–151

Dickman MB, Fluhr R (2013) Centrality of host cell death in plant-microbe interactions. Annu Rev Phytopathol **51:** 543–570

Dietz KJ (2014) Redox regulation of transcription factors in plant stress acclimation and development. Antioxid Redox Signal **21:** 1356–1372

Flors C, Fryer MJ, Waring J, Reeder B, Bechtold U, Mullineaux PM, Nonell S, Wilson MT, Baker NR (2006) Imaging the production of

singlet oxygen in vivo using a new fluorescent sensor, Singlet Oxygen Sensor Green. J Exp Bot **57:** 1725–1734

Gigon A, Matos AR, Laffray D, Zuily-Fodil Y, Pham-Thi AT (2004) Effect of drought stress on lipid metabolism in the leaves of *Arabidopsis thaliana* (ecotype Columbia). Ann Bot (Lond) **94:** 345–351

Grebner W, Stingl NE, Oenel A, Mueller MJ, Berger S (2013) Lipoxygenase6-dependent oxylipin synthesis in roots is required for abiotic and biotic stress resistance of Arabidopsis. Plant Physiol **161:** 2159–2170

Gu C, Shabab M, Strasser R, Wolters PJ, Shindo T, Niemer M, Kaschani F, Mach L, van der Hoorn RAL (2012) Post-translational regulation and trafficking of the granulin-containing protease RD21 of *Arabidopsis thaliana*. PLoS One **7:** e32422

Gutiérrez J, González-Pérez S, García-García F, Daly CT, Lorenzo O, Revuelta JL, McCabe PF, Arellano JB (2014) Programmed cell death activated by Rose Bengal in *Arabidopsis thaliana* cell suspension cultures requires functional chloroplasts. J Exp Bot **65:** 3081–3095

Hara-Nishimura I, Hatsugai N (2011) The role of vacuole in plant cell death. Cell Death Differ **18:** 1298–1304

Hara-Nishimura I, Hatsugai N, Nakaune S, Kuroyanagi M, Nishimura M (2005) Vacuolar processing enzyme: an executor of plant cell death. Curr Opin Plant Biol **8:** 404–408

Hatsugai N, Kuroyanagi M, Yamada K, Meshi T, Tsuda S, Kondo M, Nishimura M, Hara-Nishimura I (2004) A plant vacuolar protease, VPE, mediates virus-induced hypersensitive cell death. Science **305:** 855–858

Hiruma H, Katakura T, Takenami T, Igawa S, Kanoh M, Fujimura T, Kawakami T (2007) Vesicle disruption, plasma membrane bleb formation, and acute cell death caused by illumination with blue light in acridine orange-loaded malignant melanoma cells. J Photochem Photobiol B **86:** 1–8

Hodges DM, DeLong JM, Forney CF, Prange RK (1999) Improving the thiobarbituric acid-reactive-substances assay for estimating lipid peroxidation in plant tissues containing anthocyanin and other interfering compounds. Planta **207:** 604–611

Ishibashi T, Lee CI, Okabe E (1996) Skeletal sarcoplasmic reticulum dysfunction induced by reactive oxygen intermediates derived from photoactivated rose bengal. J Pharmacol Exp Ther **277:** 350–358

Ito T (1978) Cellular and subcellular mechanisms of photodynamic action: the $^1O_2$ hypothesis as a driving force in recent research. Photochem Photobiol **28:** 493–508

Iwase H, Takatori T, Sakurada K, Nagao M, Niijima H, Matsuda Y, Kobayashi M (1998) Calcium is required for quasi-lipoxygenase activity of hemoproteins. Free Radic Biol Med **25:** 943–952

Kanofsky JR, Axelrod B (1986) Singlet oxygen production by soybean lipoxygenase isozymes. J Biol Chem **261:** 1099–1104

Khan AU, Kasha M (1994) Singlet molecular oxygen in the Haber-Weiss reaction. Proc Natl Acad Sci USA **91:** 12365–12367

Kim C, Apel K (2013) Singlet oxygen-mediated signaling in plants: moving from *flu* to wild type reveals an increasing complexity. Photosynth Res **116:** 455–464

Kim C, Meskauskiene R, Apel K, Laloi C (2008) No single way to understand singlet oxygen signalling in plants. EMBO Rep **9:** 435–439

Kim C, Meskauskiene R, Zhang S, Lee KP, Lakshmanan Ashok M, Blajecka K, Herrfurth C, Feussner I, Apel K (2012) Chloroplasts of Arabidopsis are the source and a primary target of a plant-specific programmed cell death signaling pathway. Plant Cell **24:** 3026–3039

Klotz LO, Kröncke KD, Sies H (2003) Singlet oxygen-induced signaling effects in mammalian cells. Photochem Photobiol Sci **2:** 88–94

Knight H, Trewavas AJ, Knight MR (1997) Calcium signalling in Arabidopsis thaliana responding to drought and salinity. Plant J **12:** 1067–1078

Krieger-Liszkay A, Fufezan C, Trebst A (2008) Singlet oxygen production in photosystem II and related protection mechanism. Photosynth Res **98:** 551–564

Kukreja RC, Hess ML (1992) The oxygen free radical system: from equations through membrane-protein interactions to cardiovascular injury and protection. Cardiovasc Res **26:** 641–655

Kuriyama H (1999) Loss of tonoplast integrity programmed in tracheary element differentiation. Plant Physiol **121:** 763–774

Kuriyama H, Fukuda H (2002) Developmental programmed cell death in plants. Curr Opin Plant Biol **5:** 568–573

Laloi C, Havaux M (2015) Key players of singlet oxygen-induced cell death in plants. Front Plant Sci **6:** 39

Lampl N, Alkan N, Davydov O, Fluhr R (2013) Set-point control of RD21 protease activity by AtSerpin1 controls cell death in Arabidopsis. Plant J **74:** 498–510

Lampl N, Budai-Hadrian O, Davydov O, Joss TV, Harrop SJ, Curmi PM, Roberts TH, Fluhr R (2010) Arabidopsis AtSerpin1, crystal structure and in vivo interaction with its target protease RESPONSIVE TO DESICCATION-21 (RD21). J Biol Chem **285:** 13550–13560

Lee KP, Kim C, Landgraf F, Apel K (2007) EXECUTER1- and EXECUTER2-dependent transfer of stress-related signals from the plastid to the nucleus of *Arabidopsis thaliana*. Proc Natl Acad Sci USA **104:** 10270–10275

Macri F, Vianello A (1979) Photodynamic activity of cercosporin on plant tissues. Plant Cell Environ **2:** 267–271

Matheson IBC, Etheridge RD, Kratowich NR, Lee J (1975) The quenching of singlet oxygen by amino acids and proteins. Photochem Photobiol **21:** 165–171

Meskauskiene R, Nater M, Goslings D, Kessler F, op den Camp R, Apel K (2001) FLU: a negative regulator of chlorophyll biosynthesis in *Arabidopsis thaliana*. Proc Natl Acad Sci USA **98:** 12826–12831

Mittler R (2002) Oxidative stress, antioxidants and stress tolerance. Trends Plant Sci **7:** 405–410

Miyamoto S, Ronsein GE, Prado FM, Uemi M, Corrêa TC, Toma IN, Bertolucci A, Oliveira MCB, Motta FD, Medeiros MHG, Mascio PD (2007) Biological hydroperoxides and singlet molecular oxygen generation. IUBMB Life **59:** 322–331

Mor A, Koh E, Weiner L, Rosenwasser S, Sibony-Benyamini H, Fluhr R (2014) Singlet oxygen signatures are detected independent of light or chloroplasts in response to multiple stresses. Plant Physiol **165:** 249–261

Nakamura K, Ishiyama K, Ikai H, Kanno T, Sasaki K, Niwano Y, Kohno M (2011) Reevaluation of analytical methods for photogenerated singlet oxygen. J Clin Biochem Nutr **49:** 87–95

Nelson BK, Cai X, Nebenführ A (2007) A multicolored set of in vivo organelle markers for co-localization studies in Arabidopsis and other plants. Plant J **51:** 1126–1136

Nelson MS, Pattee HE, Singleton JA (1977) Calcium activation of peanut lipoxygenase. Lipids **12:** 418–422

Nilsson R, Merkel PB, Kearns DR (1972) Unambiguous evidence for the participation of singlet oxygen ($^1O_2$) in photodynamic oxidation of amino acids. Photochem Photobiol **16:** 117–124

Oparka KJ (1991) Uptake and compartmentation of fluorescent probes by plant cells. J Exp Bot **42:** 565–579

op den Camp RGL, Przybyla D, Ochsenbein C, Laloi C, Kim C, Danon A, Wagner D, Éva Hideg E, Göbel C, Feussner I, Nater M, Apel K (2003) Rapid induction of distinct stress responses after the release of singlet oxygen in Arabidopsis. Plant Cell **15:** 2320–2332

Ramel F, Ksas B, Akkari E, Mialoundama AS, Monnet F, Krieger-Liszkay A, Ravanat JL, Mueller MJ, Bouvier F, Havaux M (2013) Light-induced acclimation of the *Arabidopsis chlorina1* mutant to singlet oxygen. Plant Cell **25:** 1445–1462

Riske KA, Sudbrack TP, Archilha NL, Uchoa AF, Schroder AP, Marques CM, Baptista MS, Itri R (2009) Giant vesicles under oxidative stress induced by a membrane-anchored photosensitizer. Biophys J **97:** 1362–1370

Roberts TH, Ahn JW, Lampl N, Fluhr R (2011) Plants and the study of serpin biology. Methods Enzymol **499:** 347–366

Steinbeck MJ, Khan AU, Karnovsky MJ (1992) Intracellular singlet oxygen generation by phagocytosing neutrophils in response to particles coated with a chemical trap. J Biol Chem **267:** 13425–13433

Triantaphylidès C, Havaux M (2009) Singlet oxygen in plants: production, detoxification and signaling. Trends Plant Sci **14:** 219–228

Triantaphylidès C, Krischke M, Hoeberichts FA, Ksas B, Gresser G, Havaux M, Van Breusegem F, Mueller MJ (2008) Singlet oxygen is the major reactive oxygen species involved in photooxidative damage to plants. Plant Physiol **148:** 960–968

Wagner D, Przybyla D, op den Camp R, Kim C, Landgraf F, Lee KP, Würsch M, Laloi C, Nater M, Hideg E, Apel K (2004) The genetic basis of singlet oxygen-induced stress responses of *Arabidopsis thaliana*. Science **306:** 1183–1185

Yamashima T (2004) Ca^{2+}-dependent proteases in ischemic neuronal death: a conserved 'calpain-cathepsin cascade' from nematodes to primates. Cell Calcium **36:** 285–293